A Study of Transition to Turbulence for Incompressible Pipe Flow using a Spectral Finite Element Method

Niklas Ericsson

NO 1998-23/ISSN 0347-2809

1998
Mathematics
Department of Mathematics
Chalmers University of Technology
and Göteborg University
S-412 96 Göteborg, Sweden

Abstract

We study numerically the transition to turbulence in parallel flow using a spectral finite element method. We also present and discuss a simple ODE-model with certain features of the transition process. We finally derive an a posteriori error estimate for the numerical method.

Acknowledgements

I would like to thank

Claes Johnson, my supervisor, for all his patience and encouragement throughout my work,

Mårten Levenstam, for his assistance in the development and testing of the computer program,

my parents, for everything.

Contents

Chapter 1

Introduction

The rising smoke from a cigarette starts out following a straight, vertical line, then begins to wiggle, and eventually dissolves into a cloud (see Fig. 1.1). This is an example of transition from laminar to turbulent flow, the mathematical study of which is an important part of hydrodynamic stability. Basic questions concern the nature and the origin of the break-down from laminar to turbulent flow. In the above example, the pertinent question is why the laminar flow starts to break down at the distance d from the tip of the cigarette, and goes fully turbulent at the distance D. The scientific challenge is to theoretically predict d and D.

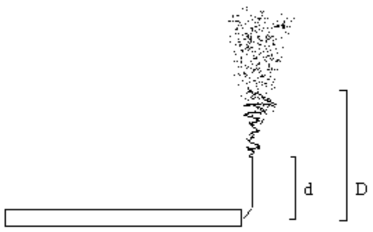

Figure 1.1: Smoke from a cigarette

The field of hydrodynamic stability originates in the nineteenth century in the work, notably of Helmholtz, Kelvin, Rayleigh and Reynolds. From his experiments on the stability of flow in a pipe [11], Reynolds observed that instability occured when a special combination of the tube radius, maximum velocity and kinematic viscosity of the water in the pipe, the Reynolds number Ua/ν, exceeded a certain value, depending on the experimental set-up.

Later, experimentalists have found transition for Reynolds numbers in the range from 2000 to 40000 at least. The effect of small disturbances on a pipe flow is still a basic element in hydrodynamic stability.

A much used method in analysing the stability of fluid flows is in terms of normal modes, and was developed already at the time of Reynolds' experiment, from the study of the stability of dynamical particle systems in mechanics. Stokes, Kelvin and Rayleigh now adapted this method to fluid dynamics. The idea is to linearise the fluid equations of motion (the Navier-Stokes equations) around a stationary, laminar solution, and study the stability with respect to each of a system of normal modes. These modes typically look like $\phi(x)\exp(\lambda t)$, where ϕ and λ are eigen-functions and eigen-values of the operator occuring in the linearised equations. If the real part of λ is positive for *some* mode, thus enabling exponential perturbation growth, then the flow is considered to be unstable. Since stability of a flow means stability with respect to an *arbitrary* (infinitesimal) perturbation, the system of normal modes should form a complete set. In practice, the method of linearisation means limitation to perturbations small compared to the laminar base flow.

Reynolds' experiment, mentioned earlier, was performed on an axisymmetric, parallel shear flow, the study of which, together with the investigation of the stability of two-dimensional parallel shear flows (with span-wise velocity and variation equal to zero), constitute a field to which much work has been devoted. The mathematical study of the stability of such flows was focussed on the two-dimensional Orr-Sommerfeld equation, derived in the beginning of this century from an assumption of span-wise constant perturbations. This is an eigen-value equation for two-dimensional perturbations. It provided a great mathematical challenge, and during the period between the twenties and the fifties, work among others by Heisenberg, Tollmien and Lin successively contributed to its analysis and understanding. The eigen-functions of the O-S operator occuring in this equation form a complete set, and the sign of the real part of the corresponding eigen-values can thus be used in the fashion described above to investigate the stability of the base flow. The two-dimensional approach was of course a simplification, but one that seemed to be justified in a theorem by Squire [12], who showed that for every three-dimensional perturbation, there exists a more unstable two-dimensional perturbation in the context of eigen-value analysis.

Still, it appeared as if something was lacking. While describing the stability properties of some flows with great accuracy, the theory failed to predict the instabilities occuring in others; for instance plane Couette and Poiseuille flows. This failure was primarily attributed to the linearisation, but a non-linear analysis discouraged through its complexity, and the interest gradually dropped.

But there was something new to retake the interest. In experiments, it had been noticed that the most observed perturbations in viscous shear flow were three-dimensional streaks, aligned in the stream-wise direction, similar to Taylor vortices between two cylinders of relative rotation, and Görtler Wirbeln in boundary layers at a concave wall. These are three-dimensional phenomena, although initially, effectively two-dimensional through their independence of the coordinate (x_1) in the stream-wise direction. They result from transient growth of initial perturbations and are 'algebraic' instabilities in contrast to exponential instabilities, considered in classical stability analysis. Though with negative real part of their eigen-values, and from a qualitative view stable in the sense that they approach zero as time tends to infinity, they can grow and reach considerable amplitudes before decay sets in, and during this time override the purely two-dimensional perturbations by orders of magnitude in strength. From a quantitative point of view, this is of great interest as a possible 'bypass' mechanism to instability. Townsend [13] as early as 1956 hypothesises the existence of such phenomena in the form of 'attached eddies' of 'elongated structure' in turbulent pipe flow. Ten years later, Bakewell and Lumley [2] found the same type of structures in the wall region, in the form of counter rotating pairs. For further early results, see [4, 10] treating the inviscid case. In the nineties, a strong interest [6, 3, 14] in such three-dimensional elongated structures and their role in hydrodynamic stability has developed, in particular fuelled by numerical experiments showing perturbation growth of the order 100-1000 for Reynolds numbers of the order 10000 for Poiseuille flow.

Mathematically, there are two reasons for the partial failure of classical stability (eigen-value) analysis. First, as already indicated, the classical analysis is purely qualitative, investigating the behaviour of perturbations as time tends to infinity. This does not properly describe cases where the operators occuring are non-normal, e.g. the O-S operator in plane Couette and Poiseuille flow. Non-normality means that the eigen-functions of the O-S operator, though forming a complete set, are not orthogonal. In this case a standard eigen-value analysis fails, since it does not account for the large transient perturbation growth that can arise when the eigenfunctions are nearly linearly dependent. The second reason is the restriction to two-dimensional flow. The operators occuring in two- and three-dimensional Couette and Poiseuille flow are both non-normal, but only the three-dimensional case appears to have the potential of large, transient perturbation growth.

In this work, which is based on [7, 8, 9], we numerically demonstrate the existence and growth of such three-dimensional stream-wise streaks mentioned above. We refer to this as the Taylor-Görtler mechanism, which, if strong enough, through non-linear interaction with weak span-wise oscillations in the stream-wise direction of the streaks, seems to be able to cause a blow-up. This second phase of the transition process is referred to as the transversal oscillation mechanism, and is characterised by larger variations of the stream-wise velocity in the stream-wise direction.

We have a dual purpose in studying the stability of fluid flow. Besides its self-evident role in transition into turbulence, quantitative estimates of hydrodynamic stability are needed in the design and analysis of finite element methods for the Navier-Stokes equations, with adaptive error control. This is because the stability affects the growth of discretisation errors introduced. There are two different stability concepts entering in these two cases, referred to as "weak" and "strong" stability respectively.

An outline of the paper is as follows: In Chapter 2 we study a simple ODE-model, where we theoretically exhibit the Taylor-Görtler mechanism and the transversal oscillations. We further demonstrate the result of a transition scenario simulation performed for a particular flow. In Chapter 3 we describe the spectral finite element method used, and we conclude in Chapter 4 with a proof of an a posteriori error estimate.

Chapter 2

A transition study

In this chapter we study the transition process for parallel channel flows governed by the incompressible Navier-Stokes equations. The equations are stated in Section 2.1, and in Section 2.2 we also derive the basic equations in the field of hydrodynamic stability. In Section 2.3 we study a simple ODE-model, where we theoretically can exhibit some characteristic features of a transition scenario, and conclude the chapter with a numerical simulation for the special case of parallel Couette flow in Section 2.4.

2.1 The Navier-Stokes equations

The fundamental underlying physical model is the incompressible Navier-Stokes equations

$$\begin{aligned}
\frac{\partial u}{\partial t} + (u \cdot \nabla)u - \nu \triangle u + \nabla p &= f, && \text{in } \Omega, t > 0, \\
\nabla \cdot u &= 0, && \text{in } \Omega, t > 0, \\
u &= g, && \text{on } \partial\Omega, t > 0, \\
u(\cdot, 0) &= u_0(\cdot), && \text{in } \Omega,
\end{aligned} \tag{2.1}$$

expressing conservation of momentum and mass. Here $u = (u_1, u_2, u_3)^T$ is the velocity field and p is the pressure of a fluid enclosed in a domain $\Omega \subset R^3$ with boundary $\partial\Omega$, and $\nu = Re^{-1}$ is the inverse of the Reynolds number, which is a non-dimensional number characteristic for a given flow problem.

Further, f, g, and u_0 are driving force data, boundary value data, and initial data respectively.

2.2 Hydrodynamic stability

The field of hydrodynamic stability concerns the stability properties of the Navier-Stokes equations, and is of fundamental importance in perturbation growth and the study of transition into turbulence. It is, however, also crucial in the way that it affects the computability of solutions to (2.1), which will be apparent from the error analysis in Chapter 4.

Our objective is to estimate the perturbation in the solution due to a perturbation of data. Let (u, p) be a solution to the incompressible Navier-Stokes equations (2.1) and let (φ, χ) be a perturbation, i. e. $(u + \varphi, p + \chi)$ is another (nearby) solution with perturbed data.

Subtracting the Navier-Stokes equations (2.1) for (u, p) from the equations for $(u + \varphi, p + \chi)$ gives

$$\begin{aligned} \tfrac{\partial \varphi}{\partial t} + (u \cdot \nabla)\varphi + (\varphi \cdot \nabla)u + & \\ +(\varphi \cdot \nabla)\varphi - \nu \triangle \varphi + \nabla \chi &= r, && \text{in } \Omega, t > 0, \\ \nabla \cdot \varphi &= 0, && \text{in } \Omega, t > 0, \\ \varphi &= 0, && \text{on } \partial\Omega, t > 0, \\ \varphi(\cdot, 0) &= \varphi_0(\cdot), && \text{in } \Omega, \end{aligned} \tag{2.2}$$

which is an initial value problem for the perturbation (φ, χ) considered. As a quantitative measure of the perturbation growth we choose here

$$C_0^s(T, u) = \frac{\|\varphi(\cdot, T)\|_{L_2(\Omega)}}{\|\varphi(\cdot, 0)\|_{L_2(\Omega)}},$$

which we refer to as the "weak" stability constant. There is a closely related concept of "strong" stability which, as mentioned above, we will return to in Chapter 4.

2.3 An ODE-model

In this section, we describe a system of three ordinary differential equations, which in [9] is introduced and studied as a model for the Navier-Stokes equations in the case of nearly parallel flow. Our objective is to sketch a transition scenario for this simple model, which is believed to have essential similarities to the transition process in parallel flow, as will be seen in the next section. For an exposition of other low-dimensional models see [1].

The ODE-model reads: Find u: $I = (0, \infty) \to R^3$ such that for $t > 0$

$$\begin{aligned} u_{1,t} - \gamma_{12}u_1u_2 - \gamma_{13}u_1u_3 + \nu u_1 &= \nu, \\ u_{2,t} + \nu u_2 &= 0, \\ u_{3,t} - \gamma_{31}\nu u_1u_3 + \bar{\nu}u_3 &= 0, \\ u(0) &= u^0, \end{aligned} \tag{2.3}$$

where the γ_{ij} are positive constants of moderate size, $\bar{\nu} = \nu(1+\gamma_{31})$, and u^0 is a given initial data. We consider (2.3) as a model for the Navier-Stokes equations in a case of nearly parallel flow in the x_1-direction, with $u_1 \sim 1$ and small transversal velocities $u_2 \sim \nu$ and $u_3 \sim \nu$.

We note that $u = \hat{u} \equiv (1, 0, 0)$ is a stationary solution of (2.3) corresponding to stationary Poiseuille or Couette flow. To study the effect on $\hat{u}$ of a small perturbation of initial data, we now consider the linearised equations linearised around the stationary state $\hat{u}$:

$$\begin{aligned} \varphi_{1,t} - \gamma_{12}\varphi_2 - \gamma_{13}\varphi_3 + \nu\varphi_1 &= 0, \ t > 0 \\ \varphi_{2,t} + \nu\varphi_2 &= 0, \ t > 0 \\ \varphi_{3,t} + \nu\varphi_3 &= 0, \ t > 0 \\ \varphi(0) &= \varphi^0. \end{aligned} \tag{2.4}$$

With $\varphi^0 = (0, \kappa\nu, \kappa\nu)$ a small perturbation of initial data where $\kappa < 1$ is a positive parameter, the solution of (2.4) is given by

$$\varphi_1(t) = (\gamma_{12} + \gamma_{13})\kappa\nu t \exp(-\nu t), \ \varphi_i(t) = \kappa\nu \exp(-\nu t), \ i = 2, 3. \tag{2.5}$$

Still following [9], we now seek to exhibit two basic mechanisms in transition processes: the Taylor-Görtler mechanism and the transversal oscillations.

From (2.5) we see that $u_1(t)$ increases approximately linearly in time, with slope proportional to ν, through the coupling with φ_2 and φ_3 in the equation for φ_1, until $t \sim \nu^{-1}$ when $\varphi_1(t) \sim \kappa(\gamma_{12} + \gamma_{13})$. This linear increase in time of $u_1(t)$ is characteristic for the action of the Taylor-Görtler mechanism. If $u_1(t)$ reaches the threshold value $\frac{1+\gamma_{31}}{\gamma_{31}}$ at some time $t = \bar{t}$, then the $u_3(t)$-component in (2.3) starts to increase. This adds to the increase of $u_1(t)$ and a finite time blow-up takes place through the coupling between u_1 and u_3 via the transversal oscillation mechanism. Since this can be expected to happen if the product $\gamma_{13}\gamma_{31}$ is large enough, where γ_{13} is related to the Taylor-Görtler mechanism and γ_{31} to the transversal oscillation mechanism, it indicates that both mechanisms are necessary in the transition process.

2.4 Numerical simulation of transition process

In this section we present the result of a numerical simulation of perturbed, parallel Couette flow, i. e. we consider as our base flow the stationary solution of (2.1) given by

$$u = (2x_2 - 1, 0, 0). \tag{2.6}$$

The perturbation equations (2.2) are then solved with 2π-periodic boundary conditions in x_1, $\Omega = [0, 2\pi] \times [0, 1] \times [0, 1]$, and $Re = \nu^{-1} = 5000$. As initial perturbation, φ_0, we introduce a small ($\sim C\nu$) transversal rotation in the form of a pair of elongated, x_1-independent rolls (see Fig. 2.1). This perturbation is intended to generate low-speed and high-speed stream-wise streaks, through the Taylor-Görtler mechanism. Since the x_1-component of the base flow (2.6) increases linearly with x_2, one would expect two high-speed streaks (marked with + in Fig. 2.1) and two low-speed streaks (marked with − in Fig. 2.1) in the φ_1-perturbation, by simply imagining the way the transversal rotation "drags" fluid particles from higher to lower speed regions, and vice-versa. In addition, we introduce a small x_1-periodic forcing term in the perturbation equation for φ_3, to exhibit the transversal oscillation mechanism coupling φ_1 and φ_3 through the terms $\varphi_3 \frac{\partial \varphi_1}{\partial x_3}$ and $(u_1 + \varphi_1)\frac{\partial \varphi_3}{\partial x_1}$.

In Fig. 2.2 the $L_2(\Omega)$-norms of the three perturbation components are shown up to the time $t = 30$, when the blow-up begins. Note the growth of φ_1, and the turning point at $t \sim 18$ when φ_3 starts to grow. In Figs. 2.3 - 2.6 we plot level surfaces of the stream-wise perturbation component at four different times. We clearly observe two high-speed streaks in the expected positions, with stream-wise direction variation increasing with time. In these

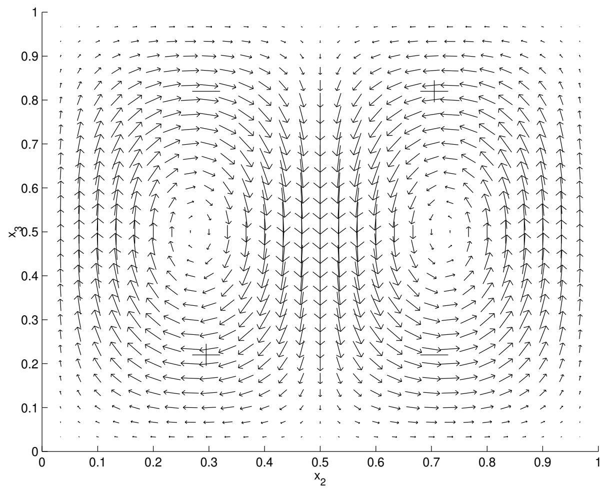

Figure 2.1: Cross-section of initial perturbation

grey-scale plots, however, the differences in magnitude of the level surfaces of φ_1 indicating its growth, cannot easily be seen.

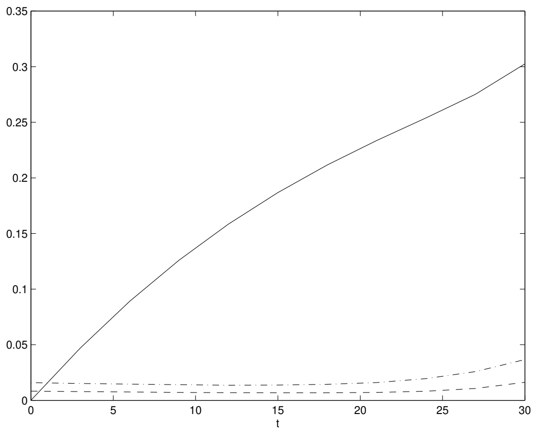

Figure 2.2: $L_2(\Omega)$-norms of φ. Solid: φ_1 Dash: φ_2 Dash-dot: φ_3

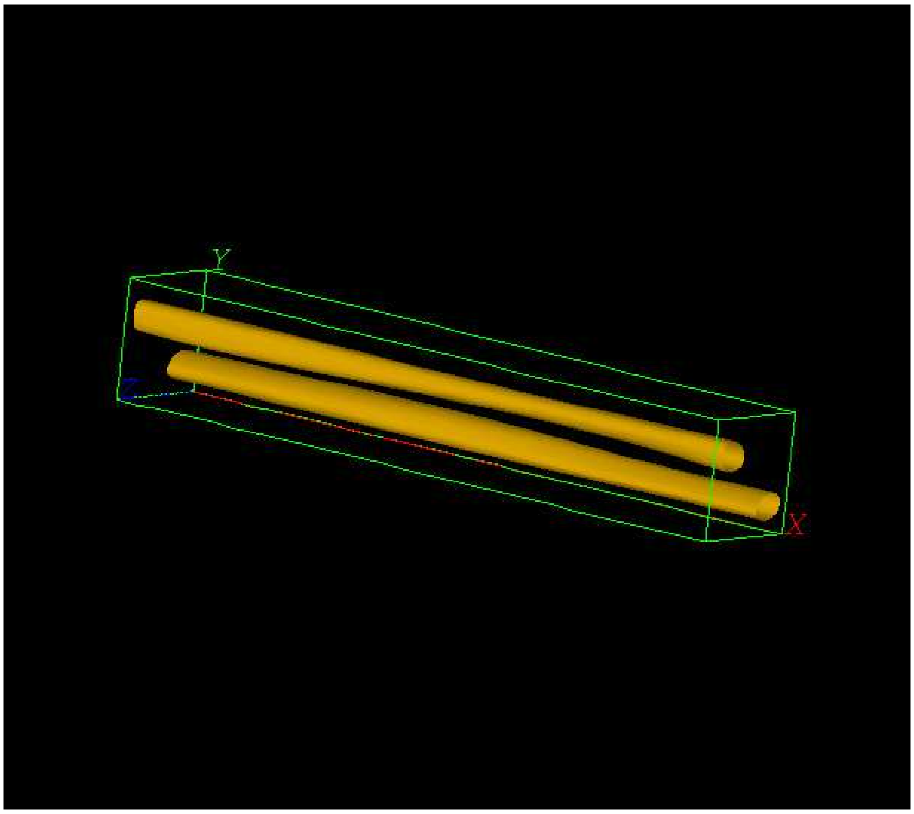

Figure 2.3: Stream-wise perturbation at t=15

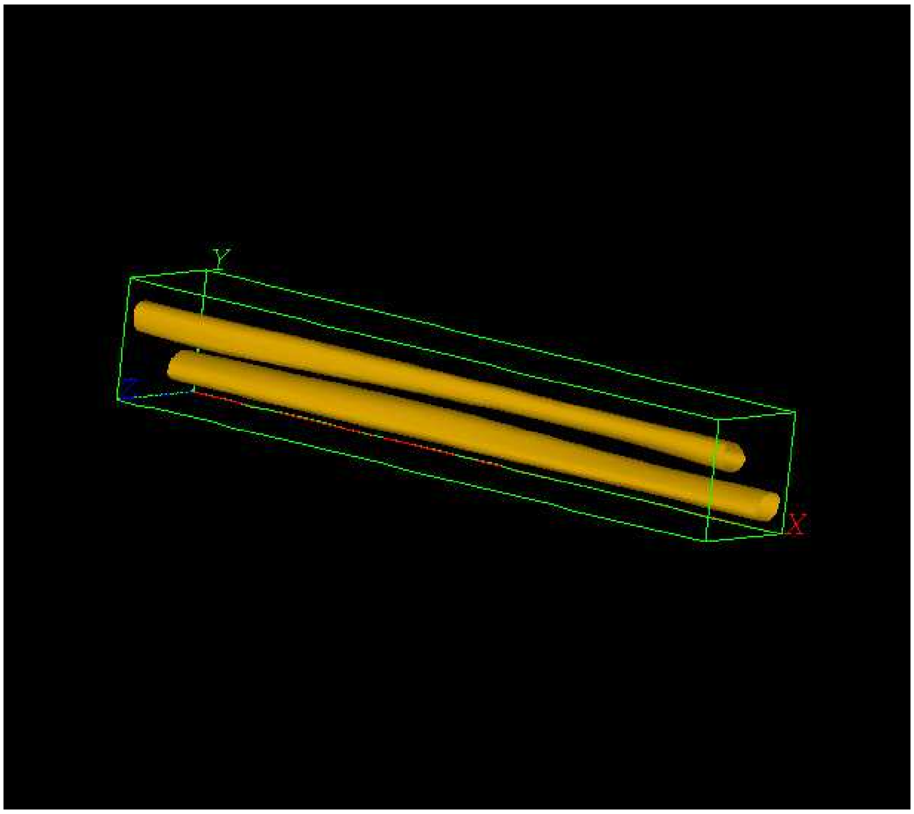

Figure 2.4: Stream-wise perturbation at t=18

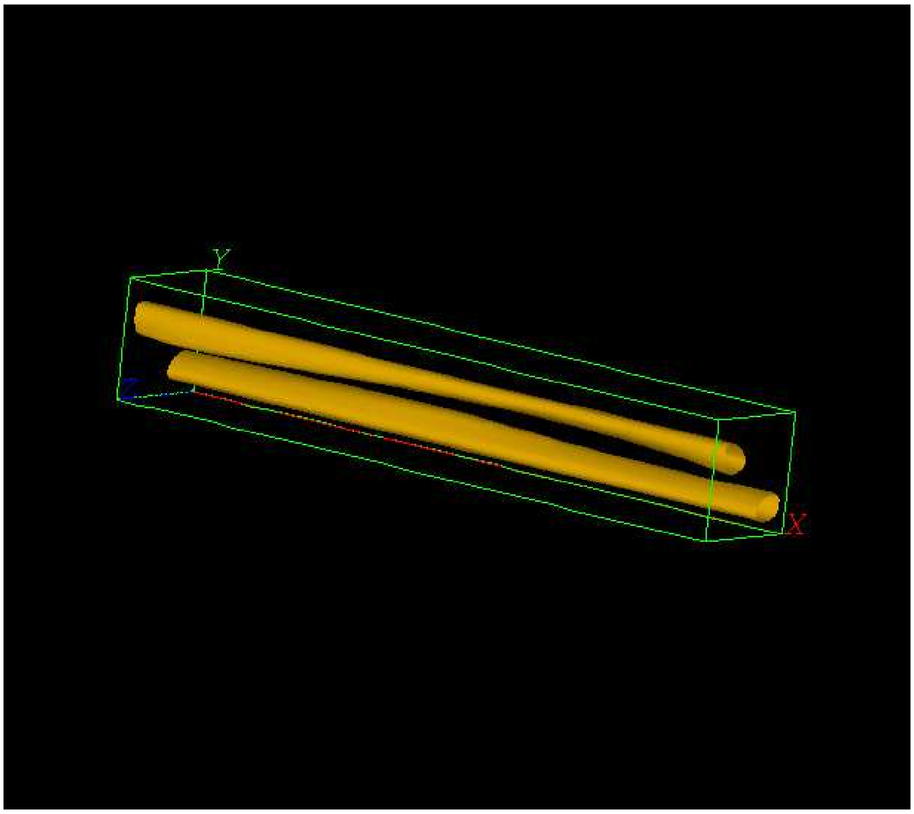

Figure 2.5: Stream-wise perturbation at t=24

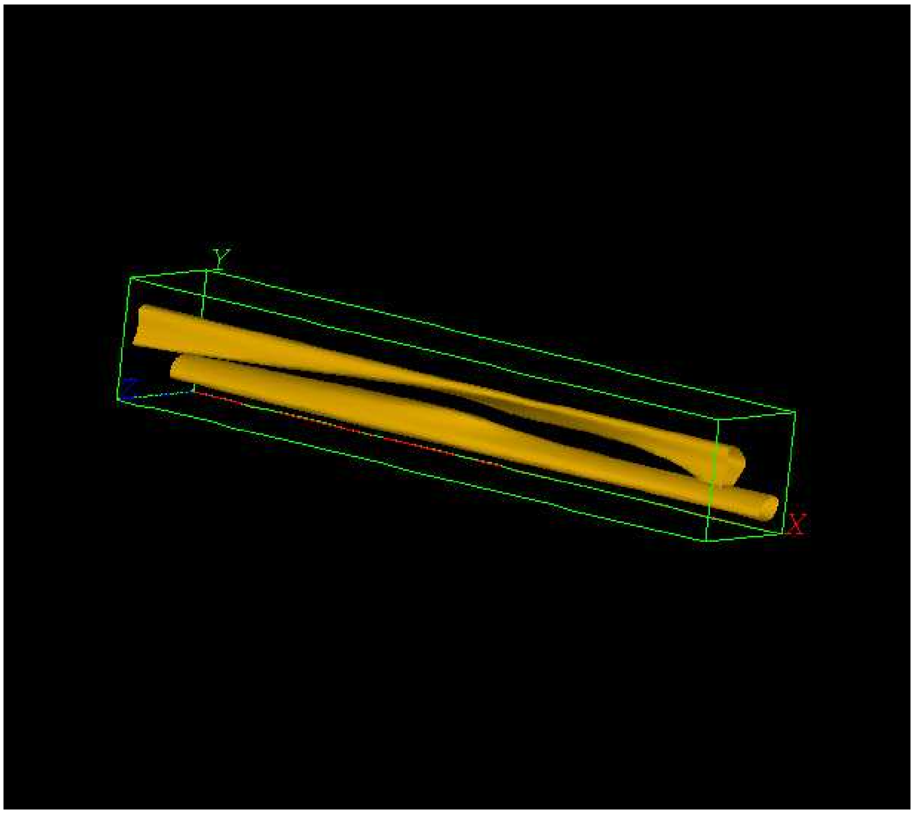

Figure 2.6: Stream-wise perturbation at t=30

Chapter 3

A spectral finite element method for the Navier-Stokes equations

In this chapter, we present a spectral finite element method for the incompressible Navier-Stokes equations. We introduce and describe different features of the method. The presentation is intentionally brief, and is intended to give a general "feeling" for the method.

3.1 General features of the method

The method uses trigonometric polynomial basis functions in one space dimension (x_1) and finite element basis functions in the other two space dimensions. This gives flexibility in geometry in the finite element directions and periodic boundary conditions in the third direction. Typical flow situations would be flow in pipes with variable cross-sections (see Fig. 3.1), or Taylor-Couette flow in the space between two coaxial cylinders. In what fol-

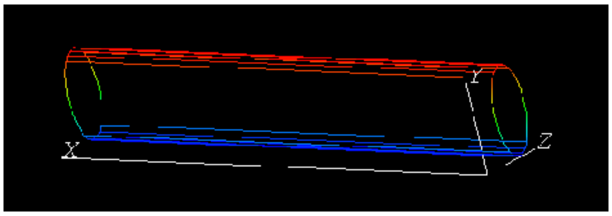

Figure 3.1: Geometry

lows we will consider the former case $\Omega = I \times \omega$, where ω is the cross-section of the pipe and $I = [0, 2\pi]$ is one period in the direction of the pipe.

3.2 Incompressibility condition

To meet the condition of incompressibility of the fluid we use the pressure correction equation

$$\begin{aligned} \triangle p &= \tfrac{1}{\delta} \nabla \cdot u, \quad \text{in } \Omega \\ \tfrac{\partial p}{\partial n} &= 0, \qquad\quad \text{on } I \times \partial\omega, \end{aligned} \tag{3.1}$$

which is solved in turns with the momentum equation. Here $\delta \propto \triangle t$ is a parameter proportional to the time step, $\triangle t$.

3.3 Discretisation in space

To discretise in space we make the Ansatz

$$u = \sum_{j=1}^{M} \sum_{k=-\frac{N}{2}}^{\frac{N}{2}-1} U_{k,j}(t) \exp(ikx_1)\, \varphi_j(x_2, x_3), \tag{3.2}$$

$$p = \sum_{j=1}^{M} \sum_{k=-\frac{N}{2}}^{\frac{N}{2}-1} P_{k,j}(t) \exp(ikx_1)\, \varphi_j(x_2, x_3), \tag{3.3}$$

where, as before, $u = (u_1, u_2, u_3)^T$ is the velocity field of the fluid and p is the pressure. Further, $\{\varphi_i\}_{i=1}^M$ is a nodal basis for the finite dimensional subspace of continuous, piecewise linear functions $V_h \subset H^1(\omega)$, and N is the (even) number of wave numbers in the x_1-direction. We use a fixed mesh which means that M and N are constant in time. Note that $U_{k,j}(t)$ are known for j:s corresponding to Dirichlet nodes on $I \times \partial\omega$, and since the pressure in (3.1) is undetermined up to an arbitrary constant we enforce $P_{0,M}(t) = 0$.

3.4 Galerkin's method

To derive the system of ordinary differential equations determining u and p in (3.2) and (3.3) respectively, we multiply the momentum equation in (2.1), and (3.1) by test functions, Ψ, integrate over Ω and finally integrate by parts to obtain the variational formulation

$$\int_\Omega \frac{\partial u_m}{\partial t}\,\Psi\,dx + \int_\Omega (u\cdot\nabla)u_m\,\Psi\,dx + \nu\int_\Omega \nabla u_m\cdot\nabla\Psi\,dx =$$

$$= -\int_\Omega \frac{\partial p}{\partial x_m}\,\Psi\,dx + \int_\Omega f_m\,\Psi\,dx, \tag{3.4}$$

$$-\int_\Omega \nabla p\cdot\nabla\Psi\,dx = \frac{1}{\delta}\int_\Omega (\nabla\cdot u)\,\Psi\,dx, \tag{3.5}$$

$\forall\,\Psi = \Psi_{k,j} = \frac{1}{2\pi}\exp(-ikx_1)\,\varphi_j$, $j = 1,\dots,M$, $k = -\frac{N}{2},\dots,\frac{N}{2}-1$, $m = 1,2,3$. Note that in (3.4) we only take $\Psi_{k,j}$ with j:s *not* corresponding to Dirichlet nodes on $I\times\partial\omega$ and that in (3.5) we exclude $\Psi_{0,M}$.

3.5 Discretisation in time

We now proceed and discretise also in time. The method uses a fixed time step, $\triangle t$, and introducing the notation $t_n = n\,\triangle t$, $n = 0,1,2,\dots$, $U^n(\cdot)\approx u(\cdot,t_n)$, $P^n(\cdot)\approx p(\cdot,t_n)$, we make the Ansatz

$$U^n = \sum_{j=1}^{M}\sum_{k=-\frac{N}{2}}^{\frac{N}{2}-1} U^n_{k,j}\exp(ikx_1)\,\varphi_j(x_2,x_3), \tag{3.6}$$

$$P^n = \sum_{j=1}^{M}\sum_{k=-\frac{N}{2}}^{\frac{N}{2}-1} P^n_{k,j}\exp(ikx_1)\,\varphi_j(x_2,x_3), \tag{3.7}$$

where the remark at the end of Section 3.3 carries over in a natural way.

3.6 Fully discrete scheme

With a one step difference approximation of the time derivative in (3.4), we finally obtain (cf. Section 3.4)

$$\int_\Omega \frac{U^n_m - U^{n-1}_m}{\triangle t}\,\Psi\,dx + \nu\int_\Omega \nabla U^n_m\cdot\nabla\Psi\,dx =$$

$$= -\int_\Omega (U^{n-1}\cdot\nabla)U^{n-1}_m\,\Psi\,dx - \int_\Omega \frac{\partial P^{n-1}}{\partial x_m}\,\Psi\,dx + \int_\Omega f_m(\cdot,t_{n-1})\,\Psi\,dx, \tag{3.8}$$

$$-\int_\Omega \nabla P^{n-1} \cdot \nabla \Psi \, dx = \frac{1}{\delta} \int_\Omega (\nabla \cdot U^{n-1}) \, \Psi \, dx, \tag{3.9}$$

where, with a slight abuse of notation, $U^n = (U_1^n, U_2^n, U_3^n)^T$, $m = 1, 2, 3$, $n = 1, 2, 3, \ldots$ It is crucial that the pressure term and the non-linear term in (3.8) are evaluated at time t_{n-1} while the linear (viscous) term is evaluated at time t_n. The reason for this will be clear from Section 3.8.

3.7 Non-linear term

The non-linear term in (3.8) will involve Fourier integrals of the form

$$\frac{1}{2\pi} \int_I (\sum_{k'} c_{k'} \, \exp(ik'x_1)\,)\,(\sum_{k''} c_{k''} \, \exp(ik''x_1)\,) \exp(-ikx_1) \, dx_1,$$

with the c_k:s depending on the solution U^{n-1}. To evaluate these integrals at minimal cost the Fast Fourier Transform (FFT) is used. The idea is to first perform an inverse transform, then do multiplication in physical space and finally perform a forward transform. Since the cost of the FFT:s is $O(N \log N)$ this will improve the $O(N^2)$ cost paid for direct evaluation of the integrals. Aliasing removal is done to eliminate the aliasing error occuring.

3.8 Parallel implementation

One of the main advantages with the method is that it is easy to implement on parallel machines, which we now show. We begin re-writing (3.8) as

$$\int_\Omega U_m^n \, \Psi \, dx + \nu \, \Delta t \int_\Omega \nabla U_m^n \cdot \nabla \Psi \, dx = \int_\Omega U_m^{n-1} \, \Psi \, dx -$$

$$-\Delta t \int_\Omega (U^{n-1} \cdot \nabla) U_m^{n-1} \, \Psi \, dx - \Delta t \int_\Omega \frac{\partial P^{n-1}}{\partial x_m} \, \Psi \, dx + \Delta t \int_\Omega f_m(\cdot, t_{n-1}) \, \Psi \, dx, \tag{3.10}$$

and inserting (3.6) and (3.7) into (3.10) leads to

$$\sum_{\substack{j'=1 \\ non-D}}^{M} U_{k,j'}^n \, \{ \int_\omega \varphi_{j'} \, \varphi_j \, dx + \nu \, \Delta t \, (k^2 \int_\omega \varphi_{j'} \, \varphi_j \, dx \; + \int_\omega \bar{\nabla} \varphi_{j'} \cdot \bar{\nabla} \varphi_j \, dx) \} =$$

$$= [RHS]_{k,j}^{n-1}, \tag{3.11}$$

where $\bar{\nabla}$ denotes $(\frac{\partial}{\partial x_2}, \frac{\partial}{\partial x_3})$, $j = 1, \ldots, M$, $k = -\frac{N}{2}, \ldots, \frac{N}{2}-1$, $n = 1, 2, 3, \ldots$

According to the remark at the end of Section 3.4, we only take j:s *not* corresponding to Dirichlet nodes on $I \times \partial\omega$; also, the terms with j':s corresponding to these nodes have been moved to the right hand side. The main objective here is to show the structure of the left hand side appearing in the discrete equations and therefore the right hand side is shown schematically only. From (3.11) it is obvious that the discrete (linear) system of equations decouples into N smaller systems of equations (all with symmetric, positive definite matrices); one for each wave number, k. This fact makes parallel implementation of the step of solving the discrete equations easy to accomplish. The other time consuming step in the algorithm, computation of the right hand side, is through the process of element-wise computation and assembling also well suited for parallel implementation.

Chapter 4

An a posteriori error estimate

In this chapter, we give a proof of an a posteriori error estimate for a semi-discrete method for the incompressible Navier-Stokes equations. In Section 4.1 we give a variational formulation of the Navier-Stokes equations, which we discretise in Section 4.2, to obtain a semi-discrete method. In Section 4.3 we introduce a linearised dual continuous problem, which, using the Galerkin orthogonality, gives us an error representation in Section 4.4. We then need interpolation error estimates for the dual solution, and these are proved in Section 4.5. Finally, considering the concept of "strong" stability for the dual continuous problem, we arrive at the a posteriori error estimate in Section 4.6.

For clarity reasons, we only discretise in space, and follow closely the exposition in [8].

4.1 A variational formulation of the Navier-Stokes equations

We begin by re-stating the incompressible Navier-Stokes equations (2.1) with periodic boundary conditions in x_1, and homogeneous Dirichlet boundary conditions in x_2, x_3:

$$
\begin{aligned}
\frac{\partial u}{\partial t} + (u\cdot\nabla)u - \nu \triangle u + \nabla p &= f, && \text{in } I\times\omega\times(0,T),\\
\nabla\cdot u &= 0, && \text{in } I\times\omega\times(0,T),\\
u &= 0, && \text{on } I\times\partial\omega\times(0,T),\\
u(x_1=0,\cdot) &= u(x_1=2\pi,\cdot), && t\in(0,T),\\
\frac{\partial u}{\partial x_1}(x_1=0,\cdot) &= \frac{\partial u}{\partial x_1}(x_1=2\pi,\cdot), && t\in(0,T),\\
u(\cdot,0) &= u_0(\cdot), && \text{in } I\times\omega.
\end{aligned}
\tag{4.1}
$$

Introducing the space $\hat{V} = V\times H$, where $V = H^1((0,T);\bar{V})$ and $H = L_2((0,T);\bar{H})$, with $\bar{V} = \{v : v\in H^1[(\Omega)]^3, v = 0 \text{ on } I\times\partial\omega, v(x_1=0) = v(x_1=2\pi)\}$ and $\bar{H} = \{q : q\in L_2(\Omega)/R, q(x_1=0) = q(x_1=2\pi)\}$, we give the problem (4.1) the following variational formulation: Find $\hat{u}\equiv(u,p)\in\hat{V}$ such that

$$
(u_t, v)_{I_T} + A(u;\hat{u},\hat{v}) + (u(0),v(0)) = F(v) + (u_0, v(0)),\ \forall\hat{v}\equiv(v,q)\in\hat{V},
\tag{4.2}
$$

where $(\cdot,\cdot)$ denotes the $[L_2(\Omega)]^3$ inner product, and with $\hat{w}\equiv(w,r)\in\hat{V}$ and $I_T = (0,T)$,

$$
A(u;\hat{w},\hat{v}) = a(w,v) + b(u;w,v) - (r,\nabla\cdot v)_{I_T} + (q,\nabla\cdot w)_{I_T},
$$

$$
(v,w)_{I_T} = \int_0^T\int_\Omega v\cdot w\,dx\,dt,\ F(v) = (f,v)_{I_T},
$$

$$
a(w,v) = \nu\sum_{j=1}^{3}(\nabla w_j,\nabla v_j)_{I_T},\ b(u;w,v) = ((u\cdot\nabla)w,v)_{I_T}.
$$

4.2 A semi-discrete Galerkin method

To formulate the semi-discrete method, let $\hat{V}_{N,h} = V_{N,h}\times H_{N,h}$, where $V_{N,h} = H^1((0,T);\bar{V}_{N,h})$ and $H_{N,h} = L_2((0,T);\bar{H}_{N,h})$, with

$$
\bar{V}_{N,h} = \mathrm{span}\{\exp(ikx_1)\,\varphi_j(x_2,x_3)\}^3_{k\in J_k, j\in J_j^0}
$$

and

$$\bar{H}_{N,h} = \{q_{N,h} : q_{N,h} \in \operatorname{span}\{\exp(ikx_1)\,\varphi_j(x_2,x_3)\}_{k\in J_k, j\in J_j}, q_{N,h}(\bar{x}) = 0\}.$$

Here $\bar{x} \in \Omega$ is an arbitrary, fixed point, $J_k = \{-\frac{N}{2}, \dots, \frac{N}{2} - 1\}$ is the set of wave-numbers and $J_j = \{1, \dots, M\}$ is the set of node-numbers of a triangulation $T_h = \{K\}$ of ω into triangles K of diameter h_K, given by the "mesh function" $h(x_2, x_3) = h_K$ for $(x_2, x_3) \in K$. We assume that

$$\mu(K) \geq ch_K^2,\ K \in T_h, \tag{4.3}$$

where c is of the same order of magnitude as the minimal angle in T_h. The subset of J_j containing interior nodes only is denoted by J_j^0.

We further assume that $\{\varphi_j\}_{j\in J_j}$ is a nodal basis for the finite dimensional subspace of $H^1(\omega)$ consisting of continuous, piecewise linear polynomials on T_h. The semi-discrete formulation of (4.1) now reads: Find $\hat{u}_{N,h} \equiv (u_{N,h}, p_{N,h}) \in \hat{V}_{N,h}$ such that

$$\begin{aligned}(u_{N,h,t}, v_{N,h})_{I_T} + A(u_{N,h}; \hat{u}_{N,h}, \hat{v}_{N,h}) + (u_{N,h}(0), v_{N,h}(0)) = \\ = F(v_{N,h}) + (u_0, v_{N,h}(0)),\ \forall \hat{v}_{N,h} \equiv (v_{N,h}, q_{N,h}) \in \hat{V}_{N,h}.\end{aligned} \tag{4.4}$$

We define the error $\hat{e} \equiv (e, e_p) = (u - u_{N,h}, p - p_{N,h}) = \hat{u} - \hat{u}_{N,h} \in \hat{V}$ as the difference between the solutions of (4.2) and (4.4).

4.3 The dual problem

Omitting the quadratic term in φ, in the perturbation equations (2.2) with $r = 0$, we get the corresponding linearised perturbation equations (the linearised Navier-Stokes equations) linearised at the solution (u, p):

$$\begin{aligned}\frac{\partial\varphi}{\partial t} + (u\cdot\nabla)\varphi + (\varphi\cdot\nabla)u - \nu \triangle \varphi + \nabla\chi &= 0, && \text{in } \Omega\times(0,T),\\ \nabla\cdot\varphi &= 0, && \text{in } \Omega\times(0,T),\\ \varphi &= 0, && \text{on } \partial\Omega\times(0,T),\\ \varphi(\cdot,0) &= \varphi_0(\cdot), && \text{in } \Omega.\end{aligned} \tag{4.5}$$

In the error analysis below, an important role is played by the stability properties of the dual of (4.5), which in the periodic case is defined by

$$
\begin{aligned}
-\tfrac{\partial\varphi}{\partial t} - (u\cdot\nabla)\varphi + \nabla u_{N,h}\cdot\varphi - \\
-\nu\bigtriangleup\varphi - \nabla\chi &= 0, && \text{in } I\times\omega\times(0,T),\\
\nabla\cdot\varphi &= 0, && \text{in } I\times\omega\times(0,T),\\
\varphi &= 0, && \text{on } I\times\partial\omega\times(0,T),\\
\varphi(x_1=0,\cdot) &= \varphi(x_1=2\pi,\cdot), && t\in(0,T),\\
\tfrac{\partial\varphi}{\partial x_1}(x_1=0,\cdot) &= \tfrac{\partial\varphi}{\partial x_1}(x_1=2\pi,\cdot), && t\in(0,T),\\
\varphi(\cdot,T) &= e(\cdot,T), && \text{in } I\times\omega,
\end{aligned}
\tag{4.6}
$$

where $[(u\cdot\nabla)\varphi]_i = \sum_{j=1}^3 u_j\varphi_{i,j}$ and $[\nabla u_{N,h}\cdot\varphi]_i = \sum_{j=1}^3 \varphi_j u_{N,h\,j,i}$. Note that the dependence on u in (4.5) has been extended to a dependence also on $u_{N,h}$ in (4.6).

We conclude this section by stating a variational formulation of (4.6): Find $\hat\varphi\equiv(\varphi,\chi)\in\hat V$ such that

$$
(-\varphi_t,v)_{I_T} + L(u,u_{N,h};\hat v,\hat\varphi) + (\varphi(T),v(T)) = (e(T),v(T)),\ \forall\hat v\equiv(v,q)\in\hat V,
\tag{4.7}
$$

where

$$
L(u,u_{N,h};\hat v,\hat\varphi) =
$$

$$
= -((u\cdot\nabla)\varphi - \nabla u_{N,h}\cdot\varphi, v)_{I_T} + a(\varphi,v) + (\chi,\nabla\cdot v)_{I_T} - (q,\nabla\cdot\varphi)_{I_T}.
$$

For later use, we note that

$$
L(u,u_{N,h};\hat e,\hat\varphi) = A(u;\hat u,\hat\varphi) - A(u_{N,h};\hat u_{N,h},\hat\varphi).
\tag{4.8}
$$

4.4 Error representation

We now derive the error representation formula as follows:

$$
\|e(\cdot,T)\|^2_{L_2(\Omega)} = (e(\cdot,T),e(\cdot,T)) = (\varphi(\cdot,T),e(\cdot,T)) + (-\varphi_t,e)_{I_T} +
$$

$$
+L(u,u_{N,h};\hat e,\hat\varphi) = (\varphi(\cdot,0),e(\cdot,0)) + (e_t,\varphi)_{I_T} + A(u;\hat u,\hat\varphi) -
$$

$$
\begin{aligned}
-A(u_{N,h};\hat{u}_{N,h},\hat{\varphi}) &= F(\varphi)+(u_0(\cdot),\varphi(\cdot,0))-((u_{N,h,t},\varphi)_{I_T}+A(u_{N,h};\hat{u}_{N,h},\hat{\varphi})+\\
&+(u_{N,h}(\cdot,0),\varphi(\cdot,0))) = F(\varphi-\varphi_{N,h})+(u_0(\cdot),\varphi(\cdot,0)-\varphi_{N,h}(\cdot,0))-\\
&-((u_{N,h,t},\varphi-\varphi_{N,h})_{I_T}+A(u_{N,h};\hat{u}_{N,h},\hat{\varphi}-\hat{\varphi}_{N,h})+\\
&+(u_{N,h}(\cdot,0),\varphi(\cdot,0)-\varphi_{N,h}(\cdot,0))) = (u_0(\cdot)-u_{N,h}(\cdot,0),\varphi(\cdot,0)-\varphi_{N,h}(\cdot,0))+\\
&+(f-(u_{N,h,t}+(u_{N,h}\cdot\nabla)u_{N,h}-\nu\bigtriangleup u_{N,h}+\nabla p_{N,h}),\varphi-\varphi_{N,h})_{I_T}-\\
&-(\nabla\cdot u_{N,h},\chi-\chi_{N,h})_{I_T}+\\
&+\int_0^T\{\sum_K\int_{I\times\partial K}\frac{\nu}{2}\,h_K^{-1}\,[\frac{\partial u_{N,h}}{\partial n_K}]\cdot(\varphi-\varphi_{N,h})\,h_K\,dsdx_1\}\,dt, \qquad (4.9)
\end{aligned}
$$

where we have used (4.7) with $\hat{v}=\hat{e}$, (4.8), (4.2) with $\hat{v}=\hat{\varphi}$ and (4.4) with $\hat{v}_{N,h}=\hat{\varphi}_{N,h}$. Here $\hat{\varphi}_{N,h}\equiv(\varphi_{N,h},\chi_{N,h})\in\hat{V}_{N,h}$ is an approximation of $\hat{\varphi}$, and $[\frac{\partial u_{N,h}}{\partial n_K}]$ is the jump of the normal derivative of $u_{N,h}$ across edges of the triangles, K, in T_h.

4.5 Interpolation error estimates

In this section we prove our two main interpolation results, Theorems 4.2 and 4.3. The idea behind the proofs is to approximate functions in two steps, separating the Fourier and the piecewise polynomial approximations. We therefore begin by considering these two cases separately and our first result is

Lemma 4.1 *Suppose that f, f', ..., $f^{(p-1)}$ are 2π-periodic and that $f\in H^p(0,2\pi)$, where p is a positive integer. The Fourier approximation*

$$\tilde{f}(x_1)=\sum_{k=-N}^{N}c_k\exp(ikx_1)$$

where

$$c_k=\frac{1}{2\pi}\int_0^{2\pi}f(x_1)\exp(-ikx_1)\,dx_1$$

then satisfies

$$\|f-\tilde{f}\|_{L_2(0,2\pi)}\leq\frac{1}{(N+1)^p}\|f^{(p)}\|_{L_2(0,2\pi)}.$$

Proof: Since all series below are absolutely and uniformly convergent on $[0, 2\pi]$, we get

$$\|f - \tilde{f}\|^2_{L_2(0,2\pi)} = \int_0^{2\pi} |f - \tilde{f}|^2 \, dx_1 = \int_0^{2\pi} | \sum_{|k|>N} c_k \exp(ikx_1)|^2 \, dx_1 =$$

$$= 2\pi \sum_{|k|>N} |c_k|^2,$$

where, in the last step, we used the orthogonality of the basis functions. Letting c_k^p denote the Fourier coefficients of $f^{(p)}$, integration by parts gives the simple relation $c_k = (ik)^{-p} c_k^p$. Hence, using Parseval's equation,

$$\|f - \tilde{f}\|^2_{L_2(0,2\pi)} = 2\pi \sum_{|k|>N} \frac{1}{k^{2p}} |c_k^p|^2 \leq \frac{1}{(N+1)^{2p}} 2\pi \sum_{k=-\infty}^{\infty} |c_k^p|^2 =$$

$$= \frac{1}{(N+1)^{2p}} \int_0^{2\pi} |f^{(p)}(x_1)|^2 \, dx_1,$$

and we are done.

□

We are also going to need the following result for piecewise linear, nodal interpolation (see [5]):

Theorem 4.1 *There are interpolation error constants C_i, depending only on the minimum angle in the mesh T_h and the order of the estimate m, such that the piecewise linear nodal interpolant $\pi_h w \in V_h$ of a function w satisfies for $m = 0$ and 1,*

$$\|D^m(w - \pi_h w)\| \leq C_i \|h^{2-m} D^2 w\|,$$

where $D^1 w = Dw = \nabla w$, and

$$\|h^{-2+m} D^m(w - \pi_h w)\| + (\sum_{K \in T_h} h_K^{-3} \|w - \pi_h w\|^2_{L_2(\partial K)})^{\frac{1}{2}} \leq C_i \|D^2 w\|.$$

In the statement of Theorem 4.1, $\|\cdot\|$ denotes $\|\cdot\|_{L_2(\omega)}$. We have also introduced the notation $V_h = \text{span}\{\varphi_j(x_2, x_3)\}_{j \in J_j}$. Note that for $x \in R^n$, $D^2 w(x)$ is defined by $D^2 w(x) = (\sum_{|\alpha|=2} |D^\alpha w(x)|^2)^{\frac{1}{2}}$, where we have adopted the usual multi-index notation. Below, $\bar{D}^2 w$ denotes differentiation with respect to x_2 and x_3 only, and $\frac{\partial^2 w}{\partial x_1^2}_{av}$ is on each triangle K, with nodes N_i, N_j and N_k, defined by

$$\left.\frac{\partial^2 w}{\partial x_1^2}_{av}\right|_K = \left(\frac{\left|\frac{\partial^2 w}{\partial x_1^2}(x_1, x_2^i, x_3^i)\right|^2 + \left|\frac{\partial^2 w}{\partial x_1^2}(x_1, x_2^j, x_3^j)\right|^2 + \left|\frac{\partial^2 w}{\partial x_1^2}(x_1, x_2^k, x_3^k)\right|^2}{3} \right)^{\frac{1}{2}}$$

We are now ready to state and prove the following

Theorem 4.2 *There is an interpolation error constant C_i, depending only on the minimum angle in the mesh T_h, such that there exists an approximation $w_{N,h} \in \operatorname{span}\{\exp(ikx_1)\,\varphi_j(x_2,x_3)\}_{k\in J_k, j\in J_j}$ of a function w that satisfies*

$$\|\frac{1}{h^2+N^{-2}}(w - w_{N,h})\|_{L_2(\Omega)} \leq C_i(\|\bar{D}^2 w\|_{L_2(\Omega)} + \|\frac{\partial^2 w}{\partial x_1^2}_{av}\|_{L_2(\Omega)}).$$

Proof: First we introduce the function w_h, which for all x_1 is defined as the nodal interpolant of w, i. e.

$$w_h(x_1, x_2, x_3) = \sum_{j\in J_j} \xi_j(x_1)\varphi_j(x_2, x_3),$$

where $\xi_j(x_1) = w(x_1, x_2^j, x_3^j)$ with (x_2^j, x_3^j) being the coordinates of node j in the triangulation T_h. Using Theorem 4.1 we now estimate the error

$$\|h^{-2}(w - w_h)\|^2_{L_2(\Omega)} = \int_0^{2\pi} (\int_\omega h^{-4}|w - w_h|^2 \, dx_2 dx_3)\, dx_1 \leq$$

$$\leq C_i^2 \int_0^{2\pi} (\int_\omega (\bar{D}^2 w)^2 \, dx_2 dx_3)\, dx_1 = C_i^2 \|\bar{D}^2 w\|^2_{L_2(\Omega)},$$

which gives us the estimate

$$\|h^{-2}(w - w_h)\|_{L_2(\Omega)} \leq C_i \|\bar{D}^2 w\|_{L_2(\Omega)}.$$

We now proceed and discretise also in x_1, by defining

$$w_{N,h}(x_1, x_2, x_3) = \sum_{j\in J_j} \tilde{\xi}_j(x_1)\varphi_j(x_2, x_3),$$

where $\tilde{\xi}_j$ is the Fourier approximation of ξ_j defined by

$$\tilde{\xi}_j(x_1) = \sum_{k\in J_k} c_{j,k} \exp(ikx_1),$$

with

$$c_{j,k} = \frac{1}{2\pi} \int_0^{2\pi} \xi_j(x_1) \exp(-ikx_1)\, dx_1.$$

Applying Lemma 4.1 we can estimate the difference between w_h and $w_{N,h}$ by

$$\|N^2(w_h - w_{N,h})\|^2_{L_2(\Omega)} =$$

$$= \int_\Omega N^4 |w_h - w_{N,h}|^2\, dx = \int_\Omega N^4 |\sum_{j\in J_j} (\xi_j - \tilde{\xi}_j)\varphi_j|^2\, dx =$$

$$= \sum_{j_1,j_2\in J_j} \int_\omega \varphi_{j_1}\varphi_{j_2} (\int_0^{2\pi} N^4 (\xi_{j_1} - \tilde{\xi}_{j_1})(\bar{\xi}_{j_2} - \bar{\tilde{\xi}}_{j_2})\, dx_1)\, dx_2 dx_3 \le$$

$$\le \sum_{j_1,j_2\in J_j} (\int_\omega \varphi_{j_1}\varphi_{j_2}\, dx_2 dx_3) N^2 \|\xi_{j_1} - \tilde{\xi}_{j_1}\|_{L_2(0,2\pi)} N^2 \|\xi_{j_2} - \tilde{\xi}_{j_2}\|_{L_2(0,2\pi)} \le$$

$$\le C_i \sum_{j_1,j_2\in J_j} (\int_\omega \varphi_{j_1}\varphi_{j_2}\, dx_2 dx_3) \|\xi''_{j_1}\|_{L_2(0,2\pi)} \|\xi''_{j_2}\|_{L_2(0,2\pi)} \le$$

$$\le \frac{C_i}{2} \sum_{j_1,j_2\in J_j} (\int_\omega \varphi_{j_1}\varphi_{j_2}\, dx_2 dx_3)(\|\xi''_{j_1}\|^2_{L_2(0,2\pi)} + \|\xi''_{j_2}\|^2_{L_2(0,2\pi)}) =$$

$$= C_i \sum_{j_1,j_2\in J_j} (\int_\omega \varphi_{j_1}\varphi_{j_2}\, dx_2 dx_3) \|\xi''_{j_1}\|^2_{L_2(0,2\pi)} =$$

$$= C_i \sum_{j_1\in J_j} (\int_\omega \varphi_{j_1}\, dx_2 dx_3) \|\xi''_{j_1}\|^2_{L_2(0,2\pi)} \le$$

$$\le C_i \sum_{j\in J_j} \mu(\mathrm{supp}(\varphi_j)) \|\xi''_j\|^2_{L_2(0,2\pi)}.$$

Since, from the definition of w_h,

$$\xi''_j(x_1) = \frac{\partial^2 w}{\partial x_1^2}(x_1, x_2^j, x_3^j),$$

we conclude that

$$\|N^2(w_h - w_{N,h})\|^2_{L_2(\Omega)} \le C_i \sum_{j\in J_j} \mu(\mathrm{supp}(\varphi_j)) \| \frac{\partial^2 w}{\partial x_1^2}(\cdot, x_2^j, x_3^j)\|^2_{L_2(0,2\pi)} =$$

$$= 3C_i \sum_{K\in T_h} \mu(K) \| \left. \frac{\partial^2 w}{\partial x_1^2}_{av} \right|_K \|^2_{L_2(0,2\pi)} = 3C_i \|\frac{\partial^2 w}{\partial x_1^2}_{av}\|^2_{L_2(\Omega)},$$

and thus arrive at the estimate

$$\|N^2(w_h - w_{N,h})\|_{L_2(\Omega)} \leq C_i \, \|\frac{\partial^2 w}{\partial x_1^2}{}_{av}\|_{L_2(\Omega)}.$$

The theorem now follows by application of the triangle inequality, since

$$\|\frac{1}{h^2+N^{-2}}(w - w_{N,h})\|_{L_2(\Omega)} \leq \|\frac{1}{h^2+N^{-2}}(w - w_h)\|_{L_2(\Omega)} +$$

$$+\|\frac{1}{h^2+N^{-2}}(w_h - w_{N,h})\|_{L_2(\Omega)} \leq \|h^{-2}(w - w_h)\|_{L_2(\Omega)} +$$

$$+\|N^2(w_h - w_{N,h})\|_{L_2(\Omega)}.$$

□

To state our last interpolation result, for the "jump-term" in the error representation, we define $R_3(u_{N,h})$ by $R_3(u_{N,h})|_K = \frac{h_K^{-1}}{2} \max_{\partial K} \left|[\frac{\partial u_{N,h}}{\partial n_K}]\right|$, so that $R_3(u_{N,h})$ for a fixed value of x_1 is piecewise constant on the triangles, K, in T_h. The result now reads

Theorem 4.3 *There is an interpolation error constant C_i, depending only on the minimum angle in the mesh T_h, such that there exists an approximation $w_{N,h} \in \mathrm{span}\{\exp(ikx_1)\,\varphi_j(x_2,x_3)\}^3_{k\in J_k, j\in J_j}$ of a function w that satisfies*

$$\sum_{K\in T_h} \int_{I\times\partial K} \frac{\nu}{2}\, h_K^{-1}\, [\frac{\partial u_{N,h}}{\partial n_K}] \cdot (w - w_{N,h})\, h_K \, ds dx_1 \leq$$

$$\leq \nu C_i \, \|(h^2 + N^{-2}) R_3(u_{N,h})\|_{L_2(\Omega)} \, (\|\bar{D}^2 w\|_{L_2(\Omega)} + \|\frac{\partial^2 w}{\partial x_1^2}{}_{av}\|_{L_2(\Omega)}).$$

Proof: Following the notation in Theorem 4.2 we begin to estimate the error

$$\sum_{K\in T_h} \int_{I\times\partial K} \frac{\nu}{2}\, h_K^{-1}\, [\frac{\partial u_{N,h}}{\partial n_K}] \cdot (w - w_h)\, h_K \, ds dx_1 \leq$$

$$\leq \sum_{K\in T_h} \int_{I\times\partial K} \nu\, R_3(u_{N,h})\, |w - w_h|\, h_K \, ds dx_1 \leq$$

$$\leq \int_I \nu\, (\sum_{K\in T_h} \|(h_K^2 + N^{-2}) R_3(u_{N,h}) h_K^{1/2}\|_{L_2(\partial K)} \, \|h_K^{-3/2}(w - w_h)\|_{L_2(\partial K)})\, dx_1 \leq$$

$$\leq \int_I \nu\, (\sum_{K\in T_h} \|(h_K^2 + N^{-2}) R_3(u_{N,h}) h_K^{1/2}\|^2_{L_2(\partial K)})^{\frac{1}{2}} ($$

$$\sum_{K\in T_h} h_K^{-3}\|w-w_h\|^2_{L_2(\partial K)})^{\frac{1}{2}}dx_1.$$

Using Theorem 4.1 we can thus estimate

$$\sum_{K\in T_h}\int_{I\times\partial K}\frac{\nu}{2}\,h_K^{-1}\,[\frac{\partial u_{N,h}}{\partial n_K}]\cdot(w-w_h)\,h_K\,dsdx_1\le$$

$$\le\nu C_i\int_I(\sum_{K\in T_h}\|(h_K^2+N^{-2})R_3(u_{N,h})h_K^{1/2}\|^2_{L_2(\partial K)})^{\frac{1}{2}}\,\|\bar{D}^2w\|_{L_2(\omega)}\,dx_1\le$$

$$\le\nu\sqrt{\frac{3}{c}}\,C_i\int_I(\|(h^2+N^{-2})R_3(u_{N,h})\|_{L_2(\omega)}\,\|\bar{D}^2w\|_{L_2(\omega)})\,dx_1\le$$

$$\le\nu\sqrt{\frac{3}{c}}\,C_i\,(\int_I\|(h^2+N^{-2})R_3(u_{N,h})\|^2_{L_2(\omega)}\,dx_1)^{\frac{1}{2}}\,(\int_I\|\bar{D}^2w\|^2_{L_2(\omega)}\,dx_1)^{\frac{1}{2}}=$$

$$=\nu\sqrt{\frac{3}{c}}\,C_i\,\|(h^2+N^{-2})R_3(u_{N,h})\|_{L_2(\Omega)}\,\|\bar{D}^2w\|_{L_2(\Omega)},$$

where we used the assumption (4.3) to estimate the line integrals over ∂K.

To complete the proof we also need to estimate

$$\sum_{K\in T_h}\int_{I\times\partial K}\frac{\nu}{2}\,h_K^{-1}\,[\frac{\partial u_{N,h}}{\partial n_K}]\cdot(w_h-w_{N,h})\,h_K\,dsdx_1\le$$

$$\le\sum_{K\in T_h}\int_{I\times\partial K}\nu\,R_3(u_{N,h})\,|w_h-w_{N,h}|\,h_K\,dsdx_1\le$$

$$\le\nu\sum_{K\in T_h}\int_{\partial K}\|(h_K^2+N^{-2})R_3(u_{N,h})\|_{L_2(0,2\pi)}\,\|N^2(w_h-w_{N,h})\|_{L_2(0,2\pi)}\,h_K\,ds\le$$

$$\le\nu\sum_{K\in T_h}(\int_{\partial K}\|(h_K^2+N^{-2})R_3(u_{N,h})\|^2_{L_2(0,2\pi)}\,h_K\,ds)^{\frac{1}{2}}($$

$$\int_{\partial K}\|N^2(w_h-w_{N,h})\|^2_{L_2(0,2\pi)}\,h_K\,ds)^{\frac{1}{2}}\le$$

$$\le\nu\,(\sum_{K\in T_h}\int_{\partial K}\|(h_K^2+N^{-2})R_3(u_{N,h})\|^2_{L_2(0,2\pi)}\,h_K\,ds)^{\frac{1}{2}}($$

$$\sum_{K\in T_h}\int_{\partial K}\|N^2(w_h-w_{N,h})\|^2_{L_2(0,2\pi)}\,h_K\,ds)^{\frac{1}{2}}.$$

Here

$$\sum_{K\in T_h}\int_{\partial K}\|(h_K^2+N^{-2})R_3(u_{N,h})\|^2_{L_2(0,2\pi)}\,h_K\,ds\le$$

$$\leq \frac{3}{c}\,\|(h^2+N^{-2})R_3(u_{N,h})\|^2_{L_2(\Omega)},$$

and

$$\sum_{K\in T_h}\int_{\partial K}\|N^2(w_h-w_{N,h})\|^2_{L_2(0,2\pi)}\,h_K\,ds =$$

$$= \sum_{K\in T_h}\int_{\partial K}\|N^2(\sum_{j\in J_j}(\xi_j-\tilde{\xi}_j)\varphi_j)\|^2_{L_2(0,2\pi)}\,h_K\,ds =$$

$$= \sum_{j_1,j_2\in J_j}\sum_{K\in T_h}\int_{\partial K}\varphi_{j_1}\varphi_{j_2}(\int_0^{2\pi}N^4(\xi_{j_1}-\tilde{\xi}_{j_1})\cdot(\bar{\xi}_{j_2}-\bar{\tilde{\xi}}_{j_2})\,dx_1)\,h_K\,ds \leq$$

$$\leq \sum_{j_1,j_2\in J_j}(\sum_{K\in T_h}\int_{\partial K}\varphi_{j_1}\varphi_{j_2}\,h_K\,ds)N^2\|\xi_{j_1}-\tilde{\xi}_{j_1}\|_{L_2(0,2\pi)}N^2\|\xi_{j_2}-\tilde{\xi}_{j_2}\|_{L_2(0,2\pi)} \leq$$

$$\leq C_i\sum_{j\in J_j}(\sum_{K\in T_h}\int_{\partial K}\varphi_j\,h_K\,ds)\|\xi_j''\|^2_{L_2(0,2\pi)} \leq$$

$$\leq C_i\sum_{j\in J_j}(\sum_{K\in T_h,\,K\subset\mathrm{supp}(\varphi_j)}\int_{\partial K}h_K\,ds)\|\xi_j''\|^2_{L_2(0,2\pi)} \leq$$

$$\leq \frac{3}{c}C_i\sum_{j\in J_j}(\sum_{K\in T_h,\,K\subset\mathrm{supp}(\varphi_j)}\mu(K))\|\xi_j''\|^2_{L_2(0,2\pi)} =$$

$$= \frac{3}{c}C_i\sum_{j\in J_j}\mu(\mathrm{supp}(\varphi_j))\|\xi_j''\|^2_{L_2(0,2\pi)} = \frac{9}{c}C_i\,\|\frac{\partial^2 w}{\partial x_1^2}_{av}\|^2_{L_2(\Omega)},$$

which completes the proof of the theorem.

□

4.6 The a posteriori error estimate

We are now ready to prove the main result in this chapter. In order to do so, we need to consider the important question regarding the growth of solutions, (φ,χ), of the dual problem (4.6), and therefore define the stability constants

$$C^s_{1,1}(T,u,u_{N,h}) = \frac{\|\bar{D}^2\varphi(\cdot,0)\|_{L_2(\Omega)}+\|\frac{\partial^2\varphi}{\partial x_1^2}_{av}(\cdot,0)\|_{L_2(\Omega)}}{\|\varphi(\cdot,T)\|_{L_2(\Omega)}}, \tag{4.10}$$

$$C^s_{1,2}(T,u,u_{N,h}) = \frac{\int_0^T\nu\,(\|\bar{D}^2\varphi\|_{L_2(\Omega)}+\|\frac{\partial^2\varphi}{\partial x_1^2}_{av}\|_{L_2(\Omega)})\,dt}{\|\varphi(\cdot,T)\|_{L_2(\Omega)}}, \tag{4.11}$$

and

$$C^s_{1,3}(T,u,u_{N,h}) = \frac{\int_0^T (\|\bar{D}^2\chi\|_{L_2(\Omega)} + \|\frac{\partial^2\chi}{\partial x_1^2}{}_{av}\|_{L_2(\Omega)})\,dt}{\|\varphi(\cdot,T)\|_{L_2(\Omega)}}. \tag{4.12}$$

We refer to these stability constants, involving derivatives, as "strong" stability constants. The reason for assuming more regularity of χ than what is implicit from (4.6), is to avoid the further difficulties in interpolation arising, when the nodal values of the function to be interpolated are possibly not well defined. From a numerical point of view, we would use piecewise linear, continuous approximation of both φ and χ, as in Section 4.2.

Recalling now the error representation formula (4.9) and using the interpolation Theorems 4.2 and 4.3, we obtain

Theorem 4.4 *Let u and $u_{N,h}$ be the solutions of the exact and discrete Navier-Stokes equations (4.1) and (4.4). Then there is an interpolation error constant C_i, depending only on the minimum angle in the mesh T_h, such that*

$$\begin{gathered}
\|u(\cdot,T) - u_{N,h}(\cdot,T)\|_{L_2(\Omega)} \leq \\
\leq C_i\, C^s_{1,1}(T,u,u_{N,h})\,\|(h^2+N^{-2})(u_0(\cdot) - u_{N,h}(\cdot,0))\|_{L_2(\Omega)} + \\
+ C_i\, C^s_{1,2}(T,u,u_{N,h})\,(\nu^{-1}\max_{0\leq t\leq T}\|(h^2+N^{-2})R_1(u_{N,h})\|_{L_2(\Omega)} + \\
+ \max_{0\leq t\leq T}\|(h^2+N^{-2})R_3(u_{N,h})\|_{L_2(\Omega)}) + \\
+ C_i\, C^s_{1,3}(T,u,u_{N,h})\,\max_{0\leq t\leq T}\|(h^2+N^{-2})R_2(u_{N,h})\|_{L_2(\Omega)},
\end{gathered}$$

where

$$R_1(u_{N,h})|_K = |u_{N,h,t} + (u_{N,h}\cdot\nabla)u_{N,h} - \nu\,\triangle\, u_{N,h} + \nabla p_{N,h} - f| \ \textit{on } K,$$

$$R_2(u_{N,h}) = |\nabla\cdot u_{N,h}|,$$

$$R_3(u_{N,h})|_K = \frac{h_K^{-1}}{2}\max_{\partial K}\left|[\frac{\partial u_{N,h}}{\partial n_K}]\right| \ \textit{on } K.$$

Note that Theorem 4.4 is "abstract" in the sense that the stability constants defined by (4.10)-(4.12) have to be computed numerically by solving the dual problem (4.6), in order to get a quantitative error estimate.

Bibliography

[1] J. S. Baggett and L. N. Trefethen, *Low-dimensional models of subcritical transition to turbulence*, Center for Applied Mathematics, Cornell University.

[2] H. P. Bakewell, Jr. and J. L. Lumley, *Viscous sublayer and adjacent wall region in turbulent pipe flow*, Phys. Fluids **10** (9), 1880-9 (1967).

[3] K. M. Butler and B. F. Farrell, *Three-dimensional optimal perturbations in viscous shear flow*, Phys. Fluids A **4** (8), 1637-50 (1992).

[4] T. Ellingsen and E. Palm, *Stability of linear flow*, Phys. Fluids **18** (4), 487-8 (1975).

[5] K. Eriksson, D. Estep, P. Hansbo, and C. Johnson, *Computational Differential Equations*, Studentlitteratur, Lund, 1996.

[6] L. H. Gustavsson, *Energy growth of three-dimensional disturbances in plane Poiseuille flow*, J. Fluid Mech. **224**, 241-60 (1991).

[7] C. Johnson, R. Rannacher, and M. Boman, *Numerics and hydrodynamic stability: Towards error control in CFD*, SIAM J. Numer. Anal. **32**, 1058-1079 (1995).

[8] C. Johnson and R. Rannacher, *On Error Control in CFD*, Preprint 1994-07, Department of Mathematics, Chalmers University of Technology, 1994.

[9] C. Johnson, R. Rannacher, and M. Boman, *On transition to turbulence and error control in CFD*, Preprint 1994-26, Department of Mathematics, Chalmers University of Technology, 1994.

[10] M. T. Landahl, *A note on an algebraic instability of inviscid parallel shear flows*, J. Fluid Mech. **98** (2), 243-51 (1980).

[11] O. Reynolds, *An experimental investigation of the circumstances which determine whether the motion of water shall be direct or sinuous, and of the law of resistance in parallel channels,* Phil. Trans. Roy. Soc. **174**, 935-82 (1883).

[12] H. B. Squire, *On the stability of three-dimensional disturbances of viscous flow between parallel walls*, Proc. Roy. Soc. A **142**, 621-8 (1933).

[13] A. A. Townsend, *The structure of turbulent shear flow*, Cambridge University Press, Cambridge (1956).

[14] L. N. Trefethen, A. E. Trefethen, S. C. Reddy, and T. A. Driscoll, *A new direction in hydrodynamic stability: Beyond eigenvalues*, Technical Report CTC92TR115 12/92, Cornell Theory Center, Cornell University (1992).